EVALUATION OF IMAGE QUALITY AND RADIATION DOSE ON GOLD NANOPARTICLES AND OTHER CLINICAL CONTRAST AGENTS IN ABDOMINAL COMPUTED TOMOGRAPHY PHANTOM

NUR JIHAN BINTI MOHD ZUKHI

UNIVERSITI SAINS MALAYSIA

2018

EVALUATION OF IMAGE QUALITY AND RADIATION DOSE ON GOLD NANOPARTICLES AND OTHER CLINICAL CONTRAST AGENTS IN ABDOMINAL COMPUTED TOMOGRAPHY PHANTOM

by

NUR JIHAN BINTI MOHD ZUKHI

**Thesis submitted in fulfillment of the requirements
for the degree of
Master of Science**

July 2018

ACKNOWLEDGEMENT

In addition, I would like to thank Ministry of Higher Education for giving me MyBrain15 (MyMaster) scholarship during my study.

Finally, I wish to express my sincere gratitude to my beloved family and teammates, Nur Diana, Noorfatin Aida, Moayyad, Norain, Lay Yean, and Zuraida, whose gave me the support and exchanged the knowledge throughout my study.

TABLE OF CONTENTS

LIST OF TABLES

LIST OF FIGURES

LIST OF ABBREVIATIONS

Al_2O_3: C	Aluminium oxide doped with carbon
AMDI	Advanced Medical and Dental Institute
AuNP	Gold nanoparticles
$BaSO_4$	Barium sulfate
CNR	Contrast-to-noise ratio
CNRD	Dose-weighted contrast-to-noise ratio
CT	Computed tomography
CTDI	Computed tomography dose index
CW-OSL	Continuous wave optically stimulated luminescence
DE	Dual-energy
DECT	Dual-energy computed tomography
DLP	Dose length product
DOSL	Delayed optically stimulated luminescence
DQE	Detective quantum efficiency
GI	Gastrointestinal
$HAuCl_4$	Chloroauric acid
LED	Light-emitting diode
LiF	Lithium fluoride
Mg	Magnesium
MNA	Malaysian Nuclear Agency

MSCT	Multislice computed tomography
MTF	Modulation transfer function
$NaBH_4$	Sodium borohydride
NPS	Noise power spectrum
OSL	Optically stimulated luminescence
OSLD	Optically stimulated luminescence dosimeter
PBS	Phosphate-buffer saline
PMMA	Polymethyl methacrylate
POSL	Pulse optically stimulated luminescence
PSF	Point spread function
ROI	Region of interest
SECT	Single-energy computed tomography
SNR	Signal-to-noise ratio
SPR	Surface plasmon resonance
TEM	Transmission electron microspopy
Ti	Titanium
TL	Thermoluminescence
TLD	Thermoluminescence dosimeter
UV-vis	Ultraviolet-visible

PENILAIAN KUALITI IMEJ DAN DOS SINARAN TERHADAP ZARAH-ZARAH NANO EMAS DAN AGEN KONTRAS KLINIKAL YANG LAIN DALAM FANTOM ABDOMEN TOMOGRAFI BERKOMPUTER

ABSTRAK

Beberapa keadaan perubatan memerlukan pemberian pelbagai agen kontras apabila pelbagai organ sasaran diperlukan bagi pengimejan diagnostik. Pada ketika ini, tidak ada fantom abdomen yang dapat menganalisis kualiti imej pelbagai agen kontras dan dos sinaran pada masa yang sama. Oleh itu, zarah nano emas dan agen-agen kontras klinikal lain telah digunakan dalam kajian ini menggunakan satu fabrikasi fantom abdomen. Objektif kajian ini adalah untuk menilai kualiti imej dan dos sinaran dengan menggunakan beberapa agen kontras (zarah nano emas, barium, iodin, gadolinium, dan susu) dalam tomografi berkomputer fantom (CT) abdomen. Fantom abdomen dengan diameter 32 sm difabrikasi daripada polimetil metakrilat dengan lima set slot dosimeter pendarkilau rangsangan optik dan tiub agen kontras berbentuk silinder dengan diameter 6 sm yang disambung bersama. Zarah nano emas disintesis dalam bentuk nanosfera dengan saiz purata 55 nm. Kepekatan untuk zarah nano emas, barium, iodin, dan gadolinium adalah masing-masing 1.1 mgml^{-1}, 12.0 mgml^{-1}, 7.6 mgml^{-1}, and 1.6 mgml^{-1}. 35 0 mgml^{-1} (4%) lemak di dalam susu digunakan di dalam kajian ini. Tiga dosimeter pendarkilau rangsangan optik ditempatkan didalam setiap tiub agen kontras untuk mengukur dos sinaran. Fantom tersebut telah diimbas dengan pelbagai voltan tiub pada 80 kV, 120 kV, dan 140 kV dalam mod tenaga tunggal manakala hanya 80 kV dan 140 kV dalam mod dwi-tenaga. Pic ditetapkan pada 0.6

dan 1.0, dan ketebalan kepingan ditetapkan pada 3.0 mm dan 5.0 mm. Nisbah kontras-kepada-hingar semua agen kontras meningkat seiring dengan ketebalan kepingan apabila lebih banyak foton ditawan. Selain itu, dos sinaran meningkat dengan voltan tiub kerana lebih banyak foton dihasilkan. Walaubagaimanapun, dos sinaran menyusut dengan peningkatan pic kerana masa pendedahan radiasi dikurangkan. CT dwi-tenaga dan CT tenaga tunggal daripada tiub voltan 80 kV dan 140 kV, memberikan kualiti imej dan dos sinaran yang optimum pada pic 1, dan ketebalan kepingan 5 mm. Parameter pengimejan yang optimum dengan menggunakan voltan tiub 120 kV dalam mod tenaga tunggal boleh diperolehi apabila pic di tetapkan pada 0.6, dan ketebalan kepingan 5 mm. Parameter pengimejan CT yang optimum dalam kajian ini boleh digunakan untuk pengimbasan pelbagai agen kontras dalam kedua-dua mod imbasan.

EVALUATION OF IMAGE QUALITY AND RADIATION DOSE ON GOLD NANOPARTICLES AND OTHER CLINICAL CONTRAST AGENTS IN ABDOMINAL COMPUTED TOMOGRAPHY PHANTOM

ABSTRACT

Some medical conditions need multiple contrast agents' administration when multiple target organs are needed for diagnostic imaging. Currently, there is no abdominal phantom that can analyse the image quality of multiple contrast agents and radiation dose simultaneously. Thus, the gold nanoparticles and other clinical contrast agents were used in this study using a fabricated abdominal phantom. The aim of this study was to evaluate the image quality and radiation dose using several contrast agents (gold nanoparticles, barium, iodine, gadolinium, and milk) in abdominal computed tomography (CT) phantom. Abdomen phantom of 32 cm diameter was fabricated from polymethyl methacrylate with five sets of optically stimulated luminescence dosimeter slots and the cylindrical contrast agent tubes with 6 cm diameter that attached together. The gold nanoparticles contrast agent was synthesised in a nanosphere shape with the average size of 55 nm. The concentration for gold nanoparticles, barium, iodine, and gadolinium are 1.1 mgml^{-1}, 12.0 mgml^{-1}, 7.6 mgml^{-1}, and 1.6 mgml^{-1}, respectively. 35.0 mgml^{-1} (4%) fat in milk was used in this study. Three optically stimulated luminescence dosimeters were placed in each contrast agent tube to measure the radiation dose. The phantom was scanned with various tube voltage at 80 kV, 120 kV, and 140 kV in single-energy mode and tube voltage was set at 80 kV and 140 kV in dual-energy mode. The pitches were set at 0.6 and 1.0, and the

slice thickness were set at 3.0 mm and 5.0 mm. The contrast-to-noise ratio of all contrast agents increases with the increment of slice thickness as more photons are captured. Furthermore, the radiation dose increases with the increment of tube voltage because more photons were produced. However, the radiation dose decreases with the increment of pitch value because the time of the radiation exposure is reduced. The dual-energy CT and single-energy CT from 80 kV and 140 kV tube voltage, gave the optimum image quality and radiation dose at pitch of 1, and mm slice thickness of 5. The optimal imaging parameter with the use of 120 kV in single-energy mode can be obtained when pitch was set at 0.6, and slice thickness of 5 mm. The optimum CT imaging parameters from this study can be used for multiple contrast agents scanning in both scan modes.

CHAPTER 1
INTRODUCTION

1.1 Clinical and Technical Background of Study

Conventional computerised tomography (CT) is based on the attenuation of X-rays beams crossing the image object which predominant physical by the photo-electric process and Compton scattering. These factors can be differentiated from two measurements at distinct energies which called 'dual-energy' that allow the reduction of beam hardening effect. Nowadays, dual-energy is commercially implemented in CT which known as dual-energy CT (DECT) (Coursey *et al.*, 2010; Johnson, 2012; Kaza, *et al.*, 2012; Schirra *et al.*, 2014). Two image datasets are acquired from DECT in the same location which allow the attenuation of different materials to be analysed. Several types of DECT scanner have commercialised nowadays, and the DECT scanner with one source and one detector which the low energy (80 kVp) and high energy (140 kVp) will be fast switched to obtain two measurements for each slice used in this study. This DECT scanner is available at Advanced Medical and Dental Institute (AMDI). This scanner gives good temporal registration between high and low energies datasets. It also has the availability of 50 cm for the field of view which can be used for image analysis.

Many factors that affect the image quality and radiation dose obtained during the scanning. The factors include tube voltage, pitch, and slice thickness. The image quality is increases with the tube voltage and the slice thickness as more photons are produce and capture in the image. However, increasing the tube voltage will increase the radiation dose as more photons are expose to the patient (Goldman, 2007a). The radiation dose expose can be reduced by increasing the pitch because the table speed

during the scanning is faster which reduce the radiation exposure time. The basic technique of dual-energy is the energy dependence of the photoelectric effect and the variability of the K-edge. K-edge itself refers to the spike of attenuation that occurs at the energy levels which greater than K-shell binding energy. This is because the absorption of the photoelectric is increased at these energy levels (Coursey *et al.*, 2010; Schirra *et al.*, 2014). Thus, the elements with K-shell electron energies within the X-rays spectrum can be used as contrast agents.

Some organs have slightly similar CT attenuation value which difficult to distinguish them on the image obtain from the scanning. Thus, the contrast agent is use in the medical imaging to enhance the visualisation of the internal structure and able to distinguish the target organ with the other organs. The most relevant contrast agent that can be used for medical X-rays imaging are the elements that have the K-edge discontinuity well inside the energy (Schirra *et al.*, 2014). Contrast material criteria must have the physical characteristics that give higher K-edge energy, non-toxicity, high circulation time, and high uptake (absorption) by the target tissue. These characteristics affect the image quality and diagnostic efficiency when using multiple contrast agents which is very important to provide the significant for clinical application (Ducote *et al.*, 2011; He *et al.*, 2012; Ghadiri *et al.*, 2013).

Higher atomic number of the contrast agent more preferable for diagnostic. This is because the photon starvation due to beam hardening is less severe than the contrast agent with the low atomic number (He *et al.*, 2012). The potential contrast agents that widely used are iodine, gadolinium, and barium. Iodine and gadolinium are administered by injecting into vein while barium is administered by mouth or enema. The nanoparticles contrast agents nowadays are rapidly growing in diagnostic field as

they give more advantages as they have small size particles. The diagnostic efficacy of nanoparticles contrast agents is higher than current contrast agents in the context of molecular imaging. There are two parameters from contrast agent that affect the image quality and diagnostic efficiency which are the energy of K-edge and absorption jump ratio. These parameters play an important role when multiple contrast agents are used simultaneously (Feuerlein *et al.*, 2008; Schlomka *et al.*, 2008; Ghadiri *et al.*, 2013). The linear attenuation coefficient (LAC) was decreasing when photon energy increased within the diagnostic X-rays energy range. However, the LAC will suddenly increase at K-edge.

Gold (Z = 79) nanoparticles is introduced as contrast agent since decade as it has all the criteria of the contrast element. Furthermore, gold is less toxic than other metal nanoparticles (Heath and Davis, 2008). Research on gold nanoparticles as contrast agent is still ongoing and more researchers came out with a new methods to improve the application of gold nanoparticles as contrast agent. Gold nanoparticles have been applied in animal studies and cell studies but not in human yet because more safety evidences are needed as it involves human life (Fan *et al.*, 2009; Reuveni, Motiei and Popovtzer, 2011; Dorsey *et al.*, 2013). The circulation time for gold is up to 15 hours which is longer than iodine (less than 10 minutes). Gold also easy to fabricate into nanoparticles with various shapes and sizes. The K-absorption edge of the gold is 80.7 keV which suits with high beam energies used in DECT (Ducote *et al.*, 2011; He *et al.*, 2012).

The shape, size, and concentration of the gold nanoparticles affect the uptake and toxicity towards the tissue (Chithrani *et al.*, 2006; Pan *et al.*, 2007). The nanosphere shape increases the probability of the gold nanoparticles to enter the cell

compare to other shapes. Furthermore, the gold nanoparticles with a size of 50 nm have the maximum uptake and non-toxicity compared to smaller size (De Jong *et al.*, 2008; Hauck *et al.*, 2008; Sonavane *et al.*, 2008; Fratoddi *et al.*, 2015). Thus, this study synthesis the gold nanoparticles to obtain the nanosphere shape with the size range of 50 nm to 60 nm, as the commercial gold nanoparticles contrast agent is too expensive. Even though gold is expensive but the usage of gold as contrast agent is little which can save the money if synthesis it. Instead, gold nanoparticles can improve the diagnostic imaging in the future with its superior characteristics.

The minimum gold nanoparticles to be visible in CT imaging is 0.49 mgml^{-1} ~ 0.5 mgml^{-1} (Hainfeld *et al.*, 2011; Alivov *et al.*, 2014). Thus, this study used the gold nanoparticles concentration of 1 mgml^{-1} as it is affordable to prepare for 100 ml contrast agent. In addition, previous studies also showed the gold nanoparticles concentration of 1 mgml^{-1} improved the contrast on the image obtained (Xu *et al.*, 2008; Hainfeld *et al.*, 2011; Alivov *et al.*, 2014).

Other studies compared the gold nanoparticles with clinical contrast agents by using the concentration they introduced to evaluate the efficiency of the contrast agents with concentration used (Schlomka *et al.*, 2008; Shikhaliev, 2012; Ghadiri *et al.*, 2013). The concentration of the contrast agents at organ will be different from injected concentration as the contrast agents were diluted with blood. This factor may affect the X-rays attenuation occurred at organ. Thus, this study used the common clinical contrast agents which are barium, iodine, and gadolinium with at organ concentration to evaluate with the gold nanoparticles. This is because to compare the efficiency of gold nanoparticles with clinically practice contrast agents. Milk also used in this study as milk is found able to enhance the GI tract which can replace the barium.

Some medical applications using more than one contrast agent may also become relevant to diagnose the different regions. For example, enhance the vascular system by using a blood-pool agent and the soft plaque by using the targeting agent. The use of multiple contrast agents simultaneously is possible in diagnostic imaging which may reduce the diagnosis time, radiation dose, and improve specificity as well as sensitivity. Thus, this study used the gold nanoparticles, barium, iodine, gadolinium, and milk simultaneously in single-energy and dual-energy CT imaging.

The abdomen phantom was fabricated in this study for scanning all contrast agents simultaneously. In addition, an existing phantom is only applicable for measuring the radiation dose. Thus, this study fabricated an abdomen phantom to mimic adult abdomen that able to evaluate the image quality of the contrast agents and the radiation dose that may expose to the organ surrounded with contrast agent.

1.2 Motivation of Study

Previous studies done by Schlomka and co-workers (2008), Shikhaliev (2012), and Ghadiri and co-workers (2013), evaluated the image quality of the clinical contrast agents with various concentrations that they introduced. However, they did not study the clinical contrast agents of barium, gadolinium, and iodine using at organ concentration simultaneously. At organ concentration of the clinical contrast agent is needed to study the image enhancement and the dose that may exposed to the organ that surrounded with the contrast agent. The clinical contrast agents with at organ concentration were used in this study to evaluate the image quality and radiation dose that obtained from the scanning.

Furthermore, they only focused on image quality by using different energies. There are another factors that affect the image quality and radiation dose. Thus, this study used dual-energy CT scanner to evaluate the image quality and radiation dose on gold nanoparticles and other clinical contrast agents in SECT and DECT using different tube voltage, slice thickness and pitch. The optimal imaging parameters that suggested from this study can be apply when using multiple contrast agents.

Research of gold nanoparticles applications as a contrast agent are still ongoing until now. More advantages of gold nanoparticles have been found by previous researcher. Gold (Au, $Z = 79$) is a good contrast agent to differentiate the tissue that has similar density but it will increase the absorbed dose of the patient as gold nanoparticles introduced secondary electron production when the incoming photons interact with gold nanoparticles (Mcquaid *et al.*, 2016). Therefore, this study will verify the efficacy of gold as a good contrast by analysing the image quality and the dose that obtained from the scanning. In addition, the gold nanoparticles was compared with other clinical contrast agents such as iodine (I, $Z = 53$), gadolinium (Gd, $Z = 64$), barium (Ba, $Z = 56$), and milk, to study the dose enhancement when applying the contrast agent.

In addition, the exist phantom is only applicable for measuring the dose. The image quality and radiation dose that obtained when applying contrast agents cannot be analysed. Thus, this study fabricated an abdominal phantom which able to evaluate the image quality and radiation dose of multiple contrast agents simultaneously.

1.3 Objectives of Study

The main objective for this study is to evaluate the image quality and radiation dose on gold nanoparticles and other clinical contrast agents in abdominal computed tomography phantom. The specific objectives of this study are as follows:

1) To fabricate an abdominal phantom for evaluating the image quality of multiple contrast agents and radiation dose simultaneously.

2) To investigate and compare the image quality and radiation dose of gold nanoparticles and other clinical contrast agents in SECT and DECT imaging.

3) To determine the optimal slice thickness, pitch, and tube voltage for gold nanoparticles and other clinical contrast agents scanning to obtain optimum image quality and radiation dose.

1.4 Significance of Study

A fabricated abdominal phantom from this study can be used for analysing the image quality of the various solutions and measuring the radiation dose simultaneously. 32 cm diameter of the phantom mimic an adult abdomen which able to be use for any purpose of study that need to use multiple solutions. The solution is not only focus on the contrast agent but it can be anything depends on the study. The phantom is able to be used either for evaluating the image quality only or for analysing the image quality and radiation dose, simultaneously.

Furthermore, the radiation dose at the organ when applying contrast agent can be estimated from measured radiation dose in this study. Thus, the imaging parameters that recommended from this study gave the optimum radiation dose to the patient which can reduce the side effect of radiation on patient. These recommended optimal

imaging parameters gave the optimum image quality and radiation dose which help the earlier stage of the abnormality or cancer tissue will be detected.

In addition, an optimal imaging parameters should be applied when using multiple contrast agents for scanning the multiple target organs simultaneously. Specific protocol needed to acquire the good image with acceptable dose absorbed by the patient. Thus, the outcome imaging parameters from this research can enhance the diagnostic efficiency when using gold nanoparticles as contrast agent or multiple contrast agents are needed for diagnostic examination. As the image obtained by using these optimal imaging parameters is good enough to diagnose, thus, no need to repeat the scanning for many times which can be cost effective.

1.5 Scope of Study

This study evaluated the image quality and radiation dose on the gold nanoparticles and other widely used clinical contrast agents (barium, iodine, gadolinium, and milk) in diagnostic imaging. The concentration for clinical contrast agents used in this study are at organ concentration while gold nanoparticles concentration is 1.1 mgml^{-1}. The gold nanoparticles were synthesised into nanosphere shape with average size of 55 nm using sodium borohydride (NaBH$_4$) as a reducing agent. All the contrast agents were scanned simultaneously in single-energy and dual-energy CT using a fabricated abdominal phantom. Various tube voltages (80 kV, 120 kV, and 140 kV), pitches (0.6 and 1.0), and slice thicknesses (3 mm and 5 mm) were applied to analyse the image quality and radiation dose. The contrast-to-noise ratio (CNR) was calculated for evaluating the image quality while optically stimulated luminescence dosimeter (OSLD) was used to measure the radiation dose that penetrate through the contrast agent. The dose measured was done to evaluate either contrast

agents enhance the dose or not. Dose weighted contrast-to-noise ratio (CNRD) was calculated to determine the optimum imaging parameter.

1.6 Thesis Outline

The thesis is structured as follows. Chapter 1 introduces the details about this research. This chapter presents the background, motivation, and objectives of study. Furthermore, the reasons why this scope is chose for this project and the clinical significance of this study are also explained in this Chapter.

Chapter 2 focuses on the literature review related to this study. Chapter 3 explains the materials and methodology used for this research. The fabrication of abdominal phantom was described in this Chapter. This Chapter also describes a technique used to investigate and evaluate the contrast agents using single-energy and dual-energy CT with different imaging parameters applied.

Chapter 4 presents the results and discussions on the findings. The evaluation of tube voltage, pitch, and slice thickness performance which affect the image quality and radiation dose are explained in this Chapter. The radiation dose measurements are also presented in Chapter 4.

Chapter 5 concludes the findings of this study. The limitations from this study and the recommendations for future works are listed in this Chapter.

1.7 Summary

Gold nanoparticles is introduced as new contrast agent because it has all the criteria of the contrast agent. The evaluation of the image quality and radiation dose simultaneously for multiple contrast agents have not been done by other researchers which motivated this study to be done. The main objective of this study which is to evaluate the image quality and radiation dose on gold nanoparticles and other clinical contrast agents in abdominal computed tomography phantom is highlighted in this Chapter.

CHAPTER 2

THEORETICAL AND LITERATURE REVIEW

2.1 Introduction

This chapter further describes the theory and literature review of this study. It outlines the interactions of X-rays with matter, computed tomography, contrast agent in CT imaging, and gold nanoparticles as new contrast agent.

2.2 Interactions of X-rays with Matter

Attenuation occurred when the X-rays interacts with the matter. There are four fundamental interactions that may occur in matter which are photoelectric absorption, Rayleigh scattering, Compton scattering, and pair production. The interactions that are important for diagnostic with the range of energy up to 150 keV are photoelectric absorption, Compton scattering and Rayleigh scattering as shown in Figure 2.1. The pair production is essential for higher energies which are larger than two electrons rest mass energy (1.02 MeV) (Dance *et al.*, 2014).
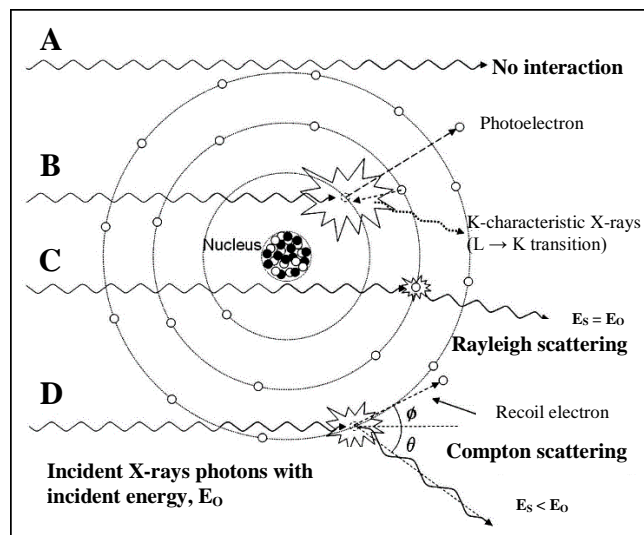
Figure 2.1 Interactions of the X-rays photon with the matter in diagnostic imaging; photoelectric absorption, Rayleigh scattering, and Compton scattering (Seibert and Boone, 2005).

The interaction that occurs in matter depends on the energy of X-rays and the electron density of the element. Each matter has a different atomic number (Z) which influence the X-rays interaction. More attenuation occur when the X-rays transverse the high absorbing material (Jensen and Wilhjelm, 2006). Figure 2.2 shows the graph of the dominant interaction depends on the atomic weight of the matter and the X-rays energy. At low photon energy with higher Z matter, the photoelectric absorption is dominant. The interaction of the Compton scattering is dominant at high photon energy (100 keV to 10 MeV) with lower Z element while the pair production is dominant at the energy above 10 MeV with higher Z element.
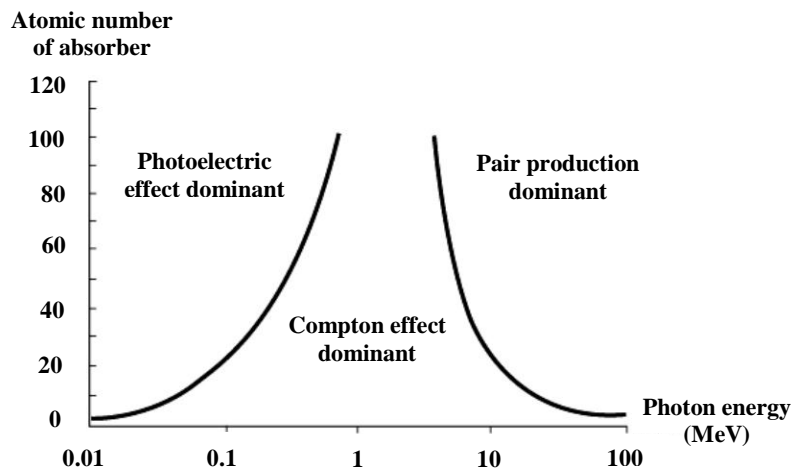
Figure 2.2 Graph of the dominant interaction that depends on the matter atomic number and the photon energy (Cherry, 2017).

2.2.1 Photoelectric absorption

Each element has a different atomic number (Z); thus the number of the electron shells and the binding energy are different. The photoelectric absorption (Figure 2.1) occurs when the incident photon interacts with an electron in the inner shell of the atom which the binding energy similar or less than the energy of an incident photon. The inner shell of the atom is also called as K-shell. The incident photon energy transfers to the K-shell electron. The electron in the inner shell is injected with

the kinetic energy which is the result of the energy absorbing from an incident photon. The injected electron is also called as photoelectron. The kinetic energy, KE, of the photoelectron is equal to:

$$KE = E_o - E_{BE} \qquad (2.1)$$

Where E_o is the incident photon energy, and E_{BE} is the binding energy of the inner electron shell.

The injected electron forms a space in the K-shell. An electron from an outer shell (L-shell) with lower binding energy filled the space in K-shell. The characteristics X-rays produced during the filling process. The energy of the produced characteristics X-rays is equal to:

$$E_{X-ray} = E_{BE(K)} - E_{BE(L)} \qquad (2.2)$$

Where E_{X-rays} is the energy of the characteristics X-rays, $E_{BE(K)}$ is the binding energy of K-shell, and $E_{BE(L)}$ is the binding energy of L-shell.

The photoelectric absorption does not occur if the incident photon energy is less than the binding energy of the K-shell. However, the rate of the photoelectric absorption decreases when the incident photon energy increases which proportional to $1/E^3$ (Connolly, 2012; Seibert and Boone, 2005). The photoelectric absorption probability to occur in matter is equal to:

$$\tau = \frac{Z^3}{E^3} \qquad (2.3)$$

Where τ is the photoelectric absorption probability, Z^3 is the cube of the matter atomic number, and E^3 is the cube of the incident photon energy.

The image contrast in the X-rays imaging is formed from the photoelectric interaction. The photoelectric effect occurs with the low incident photon energy and high Z of the element. Thus, large attenuation differences between water and bone can be seen as water has low atomic number while bone has a high atomic number. The photoelectric absorption probability of the K-shell which fill with an electron from the outer shell is known as the K absorption edge. The X-rays detector, protection devices, and contrast agent are preferable to make from the element with the high Z which has high K-shell binding energy. Thus, high energy of the characteristics X-rays produced which improve the contrast (Seibert and Boone, 2005). The contrast agents that widely used in clinical are barium, iodine, and gadolinium with the K-edge energy of 37.4 keV, 33.2 keV, and 50.2 keV, respectively.

2.2.2 Rayleigh scattering

Rayleigh scattering (Figure 2.1) also known as coherent scattering where an incident photon deflected after interacting with an electron without losing its energy. Thus, an electron is not removed from the atom. An incident photon is deflected with similar energy and different small angle from an incident photon. Thus, the scattered photon travelled forward after the interaction.

2.2.3 Compton scattering

Compton scattering is the interaction between the X-rays photon with the outermost shell of the atom as shown in Figure 2.1. An electron is injected when the incident photon energy is much higher than the outermost shell binding energy. Only the partial energy of the incident photon transfers to the electron that is injected with an angle. The remaining incident photon energy transferred as scattered X-rays which

can travel in any direction from the incident photon angle (0˚ to 180˚). However, the injected electron moved in forward direction from the incident photon angle (0˚ to 90˚) (Jensen and Wilhjelm, 2006; Seibert and Boone, 2005). The scattered photon energy is defined as the relative of the incident photon energy and the scattered photon angle as in Equation 2.4. The scattered photon energy is inversely proportional to the scattering angle.

$$\frac{E_s}{E_o} = \frac{1}{(1 + \frac{E_o}{511\ keV})(1 - \cos\theta)} \tag{2.4}$$

Where E_s is the scattered photon energy, E_o is the incident photon energy, θ is the scattering angle from the incident photon, and 511 keV is the energy of the rest mass electron. The electron rest mass energy gets from $m_o c^2$, where m_o is the mass of the rest electron (9.11 x 10^{-31} kg), and c^2 is the square of the light speed (3.0 x 10^8 ms^{-1})^2.

The image quality of the image obtained from the scanning is reduced use to the scattered X-rays. The scattered X-rays reduces the image contrast and associates to the environmental radiation because the electron was free with the scattered X-rays. The Compton scattering is dominant at high photon energy (100 keV to 10 MeV) with low Z element.

2.3 Computed Tomography

Medical imaging faces technological improvements to provide the good image quality with adequate dose exposed to the patient. The diagnostic X-rays imaging was firstly used after Wilhelm Conrad Roentgen discovered the X-rays in 1896 (Roentgen, 1896). The image produced from the X-rays is the projection of the X-rays on the object that has different absorption rates, thus, the contrast able to be seen on the film.

The technological improvements in diagnostic imaging can be seen from the earliest X-rays produced two-dimensional (2D) image also called as the radiograph. The 2D projection produced by planar X-rays radiography where the tissues are between the X-rays source and the film. Then, the computed tomography (CT) is introduced in the 1970s which produced three-dimensional (3D) image. The patient is projected with large X-rays projections at many angles around the patient. These X-rays projections are then reconstructed to form the 3D image. There are evolutions of the CT which also aim to improve the image quality with acceptable dose and reduce the scanning time.

CT is developed to overcome the limitations of the conventional radiography. In conventional radiography, the whole body thickness is projected on the film which results in the structures of the body being overlapped. Thus, radiologist is facing difficulty in distinguishing the structures from the image obtained. In addition, the conventional X-rays caused the information loss as the structures were overlapped. Multiple projections can be made in CT which improve the internal body structure and help the physicians to distinguish the structure. Moreover, the injuries and disease can be diagnosed easily, accurately and safely in CT.

An advance CT which is multislice CT (MSCT) scanner also known as spiral CT is introduced to shorten the scanning time and larger volume can be scanned. Multislice of the helical scanning can be done when the patient is moving continuously through the CT scanner gantry while the detectors and X-rays tube are rotated continuously. MSCT scanner can examine a whole body in less than 5 minutes. Besides that, the process of the image reconstruction in MSCT is faster as the software is evolved (Tsalafoutas and Koukourakis, 2010). The anatomic information with high

spatial and temporal resolution provided by CT make it as the most important tool for clinical and preclinical compared with other modalities such as magnetic resonance imaging, optical imaging, and positron emission imaging (Johnson, 2012).

However, the conventional CT also has a limitation which is unable for single-energy CT to distinguish the materials that have the same attenuation. This is because the attenuation coefficient of the material influences the intensity of the gray-scale formed from the conventional CT imaging. Thus, dual-energy CT (DECT) is introduced to overcome this limitation. DECT uses two different energies and is able to distinguish and classify the materials with the same attenuation. DECT is widely used nowadays for clinical applications such as kidney stone characterisation, bone removal and iodine quantification (Johnson *et al.*, 2007; Silva *et al.*, 2011; Kaza *et al.*, 2012). This research used DECT for evaluating the image quality and radiation dose on gold nanoparticles and other clinical contrast agents in abdominal CT phantom.

2.3.1 Basic principles of CT imaging

The X-rays source, X-rays detector, and an object or patient are the fundamental of the CT imaging. In CT, the X-rays tube and the detectors are linked and rotate around the object simultaneously as shown in Figure 2.3. Thus, projection series at the different angle are produced. In the X-rays tube, there is a high Z material which is tungsten known as an anode where the accelerated electron with high voltage hit it to produce the X-rays. The peak kilovoltage (kVp) that expressed in CT is the potential difference between the cathode and anode. The X-rays energy spectrum that generated from the X-rays tube is continuous. The X-rays filters absorb the X-rays with low energy. The low X-rays energy contribute to the patient dose which is not used for image formation as the low X-rays energy is unable to penetrate the object.

17

Thus, the CT scanner was implemented with additional filter by the manufacturers to filter out the X-rays with low energy. The detectors measure the X-rays that pass through the object. The cross-sectional images of the object areas that are obtained from the projection are reconstructed to display the image.
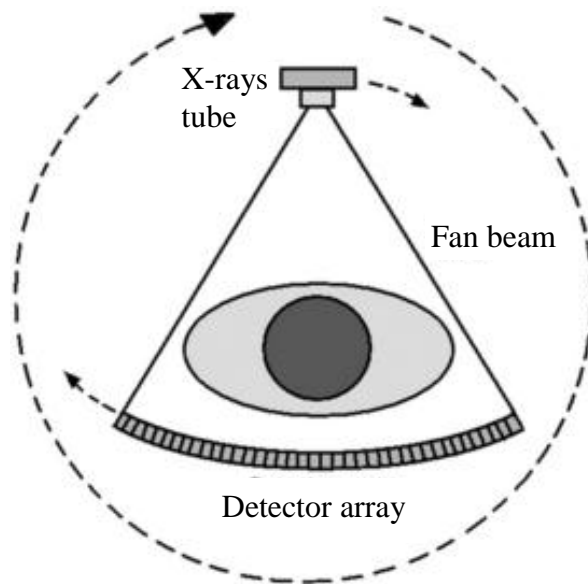
Figure 2.3 Schematic diagram of the CT scanner with the X-rays tube and large array detectors are linked (Goldman, 2007a).

CT is based on the attenuation of X-rays beams crossing the object which predominant physical by the photoelectric process and Compton scattering. These factors can be differentiated from two measurements at distinct energies which is called 'dual-energy' that allow the reduction of beam hardening effect. Nowadays dual-energy is commercially implemented in CT which known as dual-energy CT (DECT) (Coursey *et al.*, 2010; Johnson, 2012; Kaza *et al.*, 2012; Schirra *et al.*, 2014). Two image datasets are acquired from DECT in the same location which allows the analysis of energy-dependent changes in the attenuation of different materials.

There are several types of DECT scanner which the first type has one source and one detector which the low energy (80 kVp) and high energy (140 kVp) will be

fast switched to obtain two measurements for each slice (Figure 2.4A). The spectra with standard X-rays tubes have the maximum difference and least overlap when the tube voltages are set at 80 kV and 140 kV (Johnson, 2012). The tube voltage cannot be altered simultaneously for this DECT scanner. However, this scanner gives good temporal registration between high and low energies datasets. It also has the availability of 50 cm for a field of view which can be used for image analysis. This DECT scanner used in this research is available at AMDI.

A   B   C
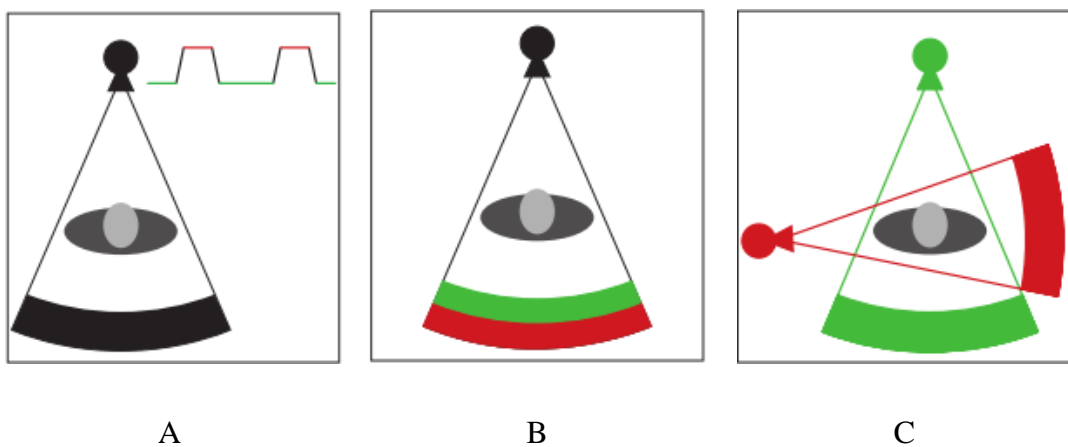
Figure 2.4 Sketch diagrams of the DECT scanner; (A) is fast switching of the tube voltage for one X-rays tube and one detector, (B) is DECT with one X-rays tube and dual layer detectors, and (C) is the DECT with two X-rays tubes and two detectors that mounted orthogonally (Johnson, 2012).

The second type of DECT scanner is a single source with dual detector layer (Figure 2.4B). This dual detector layer makes the low and high energies image datasets can be received separately where the low energy data captured by top layer while high energy data captured by bottom layer. The last type of DECT scanner is the dual source with dual detector arrays (Figure 2.4C). This scanner makes the high energy can be obtained by 120 kVp or 140 kVp and the low energy scan can be obtained simultaneously at 80 kVp or 100 kVp (Johnson, 2012; Kaza *et al.*, 2012; Schirra *et al.*,

2014). The parameters such as tube voltage, pitch, and energy affect the DECT image quality and radiation dose.

Figure 2.5 shows the X-rays spectra for 80 kVp, 120 kVp, 140 kVp and fast kilovoltage-switching of DECT. The voltage during scanning determine the maximum energy of X-rays (Lorsakul *et al.*, 2016). The mean energy is lower than the voltage applied where the mean energy for 80 kVp, 120 kVp, and 140 kVp is 44 keV, 57 keV, and 62 keV (Huda, Scalzetti and Levin, 2000). The mean energy helps the contrast agent enhancement when the K-edge energy of the contrast agent near the mean energy of the apply voltage.
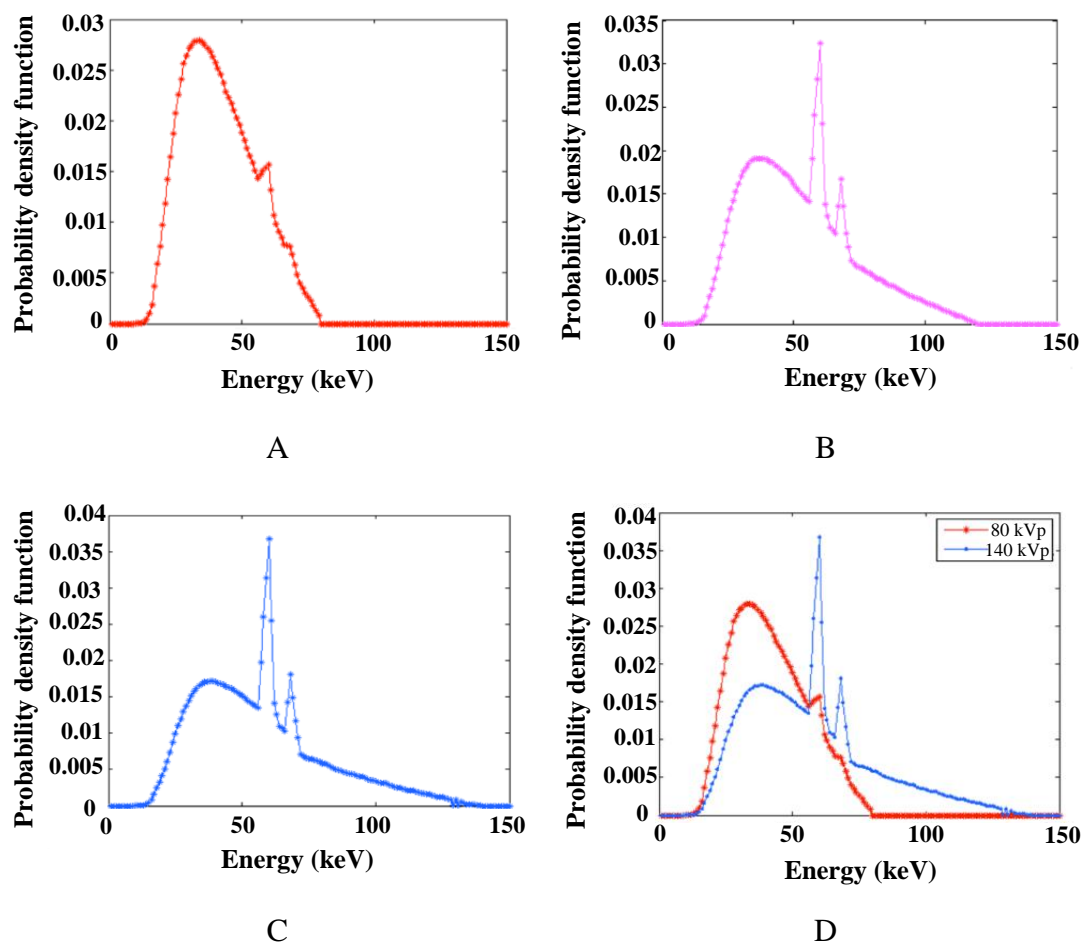

Figure 2.5 X-rays spectra for tube voltage of (A) 80 kVp, (B) 120 kVp, (C) 140 kVp, and (D) fast switching 80/140 kVp DECT (Lorsakul *et al.*, 2016).

The datasets of the X-rays attenuation profile that obtained from the scanning undergone the image reconstruction to display the images. All the projections dataset are reconstructed by applying the filtered back-projection algorithm computationally. The filtered back-projection is more effective than another algorithm and the most used algorithm (Jensen and Wilhjelm, 2006). For filtered back-projection, the raw projections are filtered before applying back-projection to reduce the blurry image. Each projection is filtered by using a suitable spatial filter, damping low spatial frequencies, and amplifying high spatial frequencies. Then, the back-projection is applied on the datasets by filling an individual projections attenuation value into each matrix cell as shown in Figure 2.6.
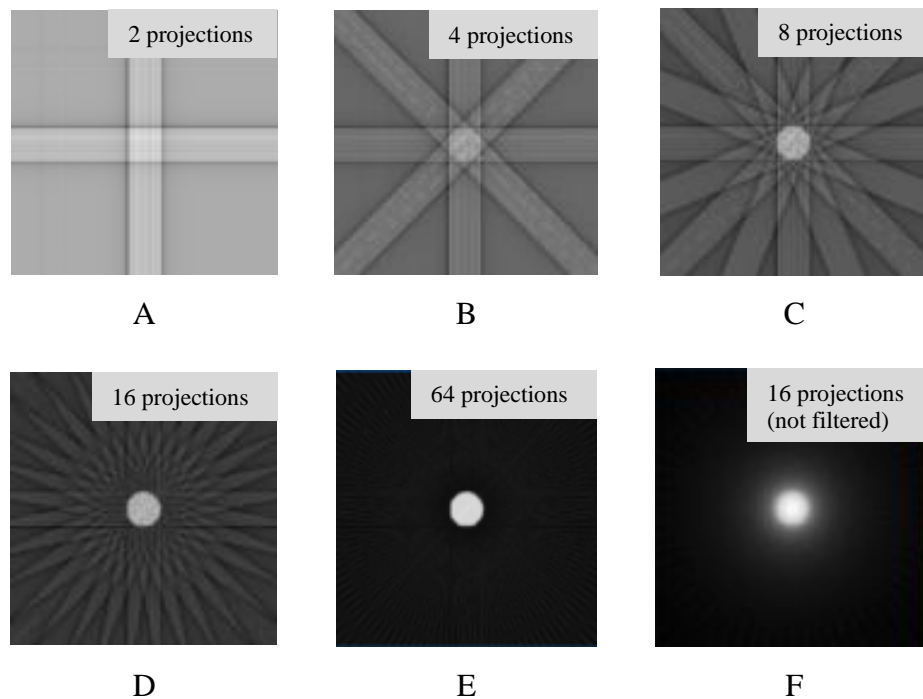

Figure 2.6 Back-projection evolution; where (A) to (E) images are obtained from the filtered projections while (F) image is obtained from the raw projections (Jensen and Wilhjelm, 2006).

A single-source CT scan (Somatom Definition; Siemens Healthcare) is used in this study. This scanner can be scanned with the low and high energy settings of 80 kV and 140 kV, respectively for DECT scanning. Tube current modulation is used for each scanning to optimise the radiation dose. Two data sets from two different X-rays energies for this DECT scanner are obtained from the sequential acquisition. Two subsequent helical scans with the stepwise table feed and the alternating tube voltages are done to reach the sequential acquisition (Johnson, 2012).

As two datasets are obtained from DECT, post-processing techniques are used to create the virtual unenhanced images (Coursey *et al.*, 2010). The attenuation differences from two energies are used for the virtual unenhanced images which also known as the fused images. *Syngo* Dual Energy software which is algorithms software that implemented with DECT scanner. The software is used for a further process of both images obtained from two tube potential to form fused images. The low image noise and normal attenuation like at tube voltage of 120 kV images are created with the weighted factor for DECT fused images (Siemens, 2008). The weighted factor for the fused image is 30% of the information from 80 kV image and 70% of the information from 140 kV image (Eusemann *et al.*, 2008).

2.3.2 CT image quality

Human tissues or any materials have different electron densities which influence the linear attenuation coefficient. More attenuations of X-rays occur in the high *Z* material which also called as high absorbing material resulting the detectors will not receive as much radiation from this material (Jensen and Wilhjelm, 2006). Thus, the bright image is formed on the film at high *Z* material region. Gray-scale images are formed from the X-rays which also display in CT.

In CT, the average X-rays attenuations of the tissues that rely on the corresponding voxel are displayed on the CT images. The CT numbers with the unit of Hounsfield Units (HU) are used to represent the tissues attenuation values on the image obtained (Hounsfield, 1973; Brooks, 1977). The CT number is defined as Equation 2.5:

$$CT\ number = \frac{\mu_x - \mu_{water}}{\mu_{water}} \times 1000\ HU \qquad (2.5)$$

Where μ_x is the tissue attenuation coefficient, and μ_{water} is the water attenuation coefficient. The lowest attenuation coefficient is air which has low density, while the highest attenuation coefficient in the body is bone as it has highest density. Thus, air has the lowest CT number which is – 1000 HU while the compact bone has the highest CT number which is up to 3000 HU. The CT number of water is 0 HU. Figure 2.7 shows the Hounsfield scale with the range from -1000 to +1000.
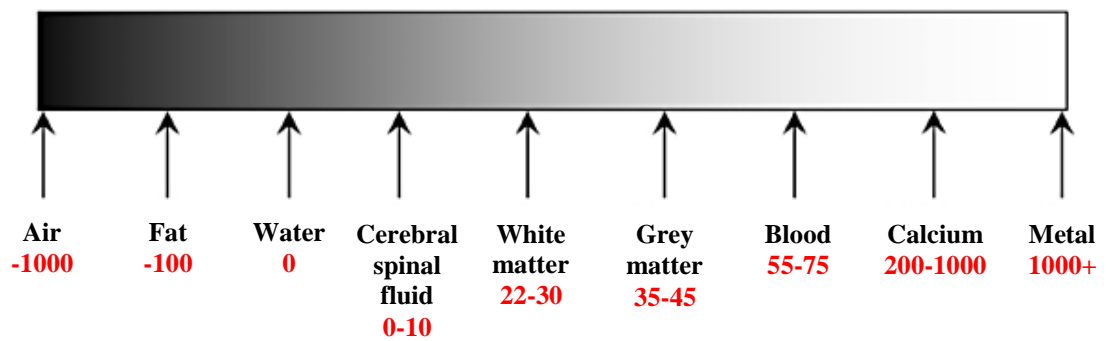

Air	Fat	Water	Cerebral spinal fluid	White matter	Grey matter	Blood	Calcium	Metal
-1000	-100	0	0-10	22-30	35-45	55-75	200-1000	1000+

Figure 2.7 The Hounsfield scale from -1000 to +1000 (Osborne *et al.*, 2016).

Several quantities that can be analysed on the image obtained from the scanning. The numbers that can be measured on the image are signal-to-noise ratio, (SNR), contrast-to-noise ratio (CNR), noise power spectrum (NPS), detective quantum efficiency (DQE), modulation transfer modulation (MTF), and point spread function (PSF) (Crop, 2015). These quantities aim to analyse the different type of image quality

either noise, spatial resolution, or image contrast. In this study, CNR is calculated to represent the image quality of the gold nanoparticles and other contrast agents. CNR is measured to evaluate the contrast of the different contrast media used for different imaging parameters.

2.3.2(a) Image contrast

The image contrast formed by the scanning is achieved from the primary X-rays. The image displayed the object scanned in the variation of the gray-scale. The average gray-scale difference between the objects defined the contrast. The contrast of the image is reduced by the scattered X-rays which introduces the signals that not represent the object scanned (Seibert and Boone, 2005).

The image obtained from the scanning is created by the detection of the incident transmitted X-rays. Transmitted X-rays are when the object X-rays attenuation coefficient modify the uniform generated X-rays beam (Jensen and Wilhjelm, 2006). The normal linear attenuation law is used for the X-rays attenuation as shown in Equation 2.6:

$$I(x) = I_0 \ e^{-\mu x} = \ I_0 \ e^{\frac{-\mu}{\rho}\rho x} \tag{2.6}$$

Where x is the distance of the X-rays transverse in the material, μ is the linear attenuation coefficient (m^{-1}). I_0 is the incident X-rays intensity at the entrance of matter, I_x is the X-rays intensity at distance x, ρ is the material density, and μ/ρ is the material mass attenuation coefficient.

The high X-rays source accelerating voltage (kV) will decrease the continuous X-rays spectrum minimum wavelength. This is because the X-rays energy is inversely